Mechanical Characterization of SAC305 and SnPb36Ag2 BGA Assemblies Under Static Flexural Loading

O. Dalverny, Prof., J. Alexis, Prof., J. Bosq

University of Toulouse; INP/ENIT; LGP Tarbes, France

P. Milesi, F. Dulondel, J.B. Libot, PhD.

SAFRAN Electronics & Defense Eragny-sur-Oise, France

ABSTRACT

Static bending-induced solder joint damage is a main reliability concern for aerospace and military industries whose Printed Circuit Board Assemblies (PCBAs) are required to remain functional under flexural loading. In order to dissipate heat in electronic assemblies, it is common to install thermal gap pads on electronic packages. When compressing thermal gap pads during the fixture process, the PCBA can bend and solder joints can therefore crack if the deflection is too important. This paper reports the durability of 96.5Sn-3.0Ag-0.5Cu (SAC305) and 62Sn-36Pb-2Ag (SnPb36Ag2) Ball Grid Array (BGA) assemblies under static flexural loading at -55°C, 20°C and 125°C. As electronic equipment can be stored at high temperature for prolonged durations, some SAC305 test vehicles were also aged at 125°C for 192 hours. For each test configuration, the bending tests were conducted at a ramp-rate of 2 mm/min and the central displacement-to-failure was measured. Finite Element Modeling (FEM) analysis was conducted considering a global-local approach and the relationship between the central displacement-to-failure and the local PCB strain near the critical solder joints was determined for each test configuration. The results give the necessary data for designers to assess whether a specific PCBA design subjected to static bending is at risk or not.

Key words: BGA, flexural loading, static, reliability.

INTRODUCTION

Electronic equipment embeds PCBAs that can be subjected to static flexural loading due to thermal gap pads used for heat dissipation. When placing such gap pads, the pressure applied on the components like Ball Grid Arrays (BGA) packages can be such that the PCBA would bend and therefore lead to solder joint damage (Figure 1.a). Another reason for PCBA static bending is the potential discrepancies between the PCBA and the housing dimensions. For instance, an electronic component with an important thickness soldered manually, i.e. without accurate control of the solder joint thickness, could eventually be in contact with the PCBA housing (Figure 1.b). Though it is rare, it can nevertheless lead to local PCBA bending and it is therefore important to address PCBA

static bending to make sure that solder joints do not sustain critical damage. With the emergence of new lead-free solders driven by the restrictions on lead and concerns for the environment and public health, there is a need for a better understanding of the static mechanical behavior of these new solder alloys, especially for the 96,5Sn-3,0Ag-0,5Cu (SAC305) composition which is widely used in the electronic industry.

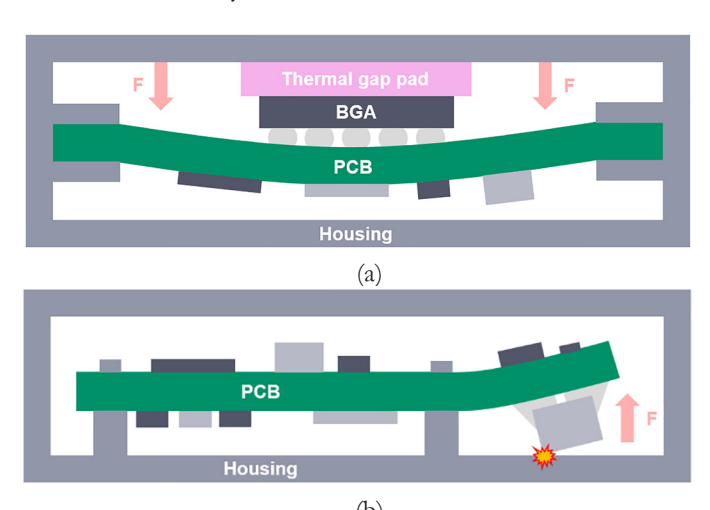


Figure 1: Flexural loading due to a) thermal gap pad and b) dimensions issues between the PCBA and the housing

Few studies have been conducted on the rupture of solder interconnects under static bending. Tan et al. performed 5-point static tests on surface mounted MCMs (Multi-Chip Modules) on PCBs at relatively low ramp-rates (0.1 to 10 mm/min) to determine the effect of PCB strain rates on the reliability of solder interconnections [1]. Their results showed that the critical solder joints located at the outermost ring were subjected to shear and tensile strains that eventually lead to intermetallic (IM) failures at the board side. Bansal et al. studied the flexural strength of BGA solder joints with ENIG (Electroless Nickel Immersion Gold) substrate surface finish using 4-point bending test at high strain rate [2]. They compared the eutectic SnPb solder with a SAC lead free solder alloy (without mentioning the exact composition).

They did not notice a significant difference between SnPb and SAC solders in the failure data. Their results showed that the PCB strain-to-failure and failure mode were dependent on the strain rate. The PCB strains measured directly with the strain gages showed that there was a linear relationship between the imposed central displacement and the PCB strain. At low strain rate (500 με/s), all of the observed failures were PCB pad lifting whereas at higher strain rates, it was a combination of brittle fracture at the component substrate ENIG interface and PCB pad lifting. Song et al. investigated the reliability under 4-point bending of BGA solder balls [3]. They showed that the PCB strain rate was a good indicator for detecting the onset of solder interconnects failure under monotonic bending tests. Though the failure analysis was not extensive, they were able to observe a copper trace failure on the PCB side. Long et al. studied the mechanical behavior of BGA packages under 4-point dynamic bending tests [4]. The failure probability plot was obtained assuming a Weibull distribution of the PCB strain-to-failure and the correlation between the experimental results and the FEM analysis allowed them to extract the details of stress and strain in the critical solder balls. The failure analysis revealed cracks in the solder joints as well as in the PCB. Recently, McCann et al. performed monotonic 4-point bending test coupled with FEM analysis in order to predict failure of flip-chip BGA at high strain rate [5]. The principal failure mode was pad cratering at the board side. Their work gave a methodology to assess the risk of BGA packages failure under monotonic bending test at high strain rate using the PCB strain as a failure criterion.

This work focuses on the static bending reliability of SAC305 and SnPb36Ag2 BGA assemblies under static flexural loading. Custom made daisy-chained BGA components have been soldered on FR-4 PCB with SAC305 and SnPb36Ag2 solder alloys and the resulting test vehicles were used for 3-point (when the load is applied on the un-populated side of the PCBA) and 4-point (when the load is applied on the populated side of the PCBA) bending tests. The static bending tests were conducted for a given ramp-rate until failure (this ramp-rate matches the speed at which the PCBA bends when placing a thermal gap pad). It was then possible to determine the central displacement-to-failure and after conducting FEM analysis, to obtain the local PCB strain-to-failure. The aim of this study is to provide numerical data of PCB strain-to-failure under static bending. When designing electronic boards with thermal gap pads, designers would therefore be able to assess whether the equipment is at risk or not.

MONOTONIC BENDING TESTS

Test Vehicles and Setup

The test vehicle consists of a 60 mm x 25 m, 2.4 mm thick FR-4 PCB on which is soldered a 25 mm x 12 mm, 1.6 mm thick custom-made BGA whose material is the same as the PCB (Figure 2.a). They are both made of a Panasonic 1755V resin with 7628 glass fibers reinforcement and have Electroless Nickel Immersion Gold (ENIG) surface finish on Solder Mask Defined (SMD) copper pads for BGA, and on Non Solder Mask Defined (NSMD) copper pads for the PCB (Figure 2.a). The PCB and the custom-made BGA are daisy-chained in order to record the electrical resistance throughout the bending test and therefore detect the failure (Figure 2.b). Two

solder alloys are considered in this study: the widely used SAC305 lead-free solder and SnPb36Ag2 for comparison.



Figure 2: Custom-made BGA assembly, a) overview, b) implementation diagram of the balls and daisy-chain

The tests are carried out using a flexural device that generates shear and tensile strain in the solder balls by a structural bending effect. The complex loading in solder balls is thus induced by the relative longitudinal displacement of the bonding surfaces, on the one hand with the substrate and on the other hand with the component. This stress can also be associated with the curvature of the substrate [6]. Two mechanical configurations will be implemented in order to simulate a curvature towards the component or towards the opposite face depending on the loading direction (Figure 3). In the most common case, for static loading, the 3-point bending test is used (Figure 3.a). In other cases, the curvature may be reversed and thus induce stresses of opposite direction in the connection. For the latter case, if the 3-point bending configuration is chosen, direct contact with the component will put the joint in compression. The configuration will then cause the cracks to re-close and make the test ineffective for the failure detection system. In order to be more representative and to be able to correctly detect the failure of the system in this configuration, we carried out tests with a 4-point bending configuration (Figure 3.b).

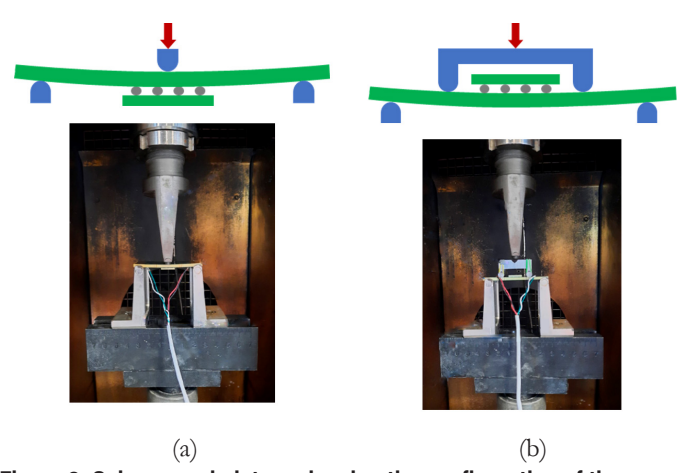


Figure 3: Scheme and picture showing the configuration of the mechanical tests according to the direction of the load, a) 3-point bending if opposite side of the component, b) 4-point bending if facing the component

This change in configuration modifies the stress in the substrate and probably in the solder balls. Preliminary numerical simulations allowed us to verify that both configurations gave the same mechanical loading in the solder ball (i.e. type of stress and level), as well as the most stressed ball being the same. This is illustrated

in Figure 4, where we can see that the stress field on the ball is shearing. For equal displacements of the loading device, the principal stresses directions are on the diagonals and the maximum stress levels are identical. However, it can be seen that between the two configurations, the areas in tension and compression are reversed. The maximum principal stress in tension is obtained for the 3-point bending while the maximum principal stress is in compression for the 4-point bending. Thus, for the latter case, the maximum tensile stress value is less than half that of the 3-point bending configuration. The 4-point bending configuration seems to be less favorable to a crack initiation and thus less critical. In both cases, the distance between the outer supports is 50 mm and for 4-point bending the distance between the two tool supports is 25 mm.

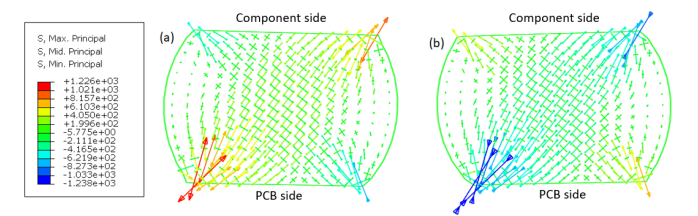


Figure 4: Comparison of the stress fields in the most stressed ball for the configurations a) 3-point bending, b) 4-point bending

Failure of assemblies corresponds to the appearance of microcracks in the solder balls or some peripheral elements leading to a degradation of the electrical continuity. Detection of failure during the test is done by measuring the voltage across the component. This is done by daisy-chain of the component connected to a dedicated electrical circuit. This circuit allows real-time monitoring of the voltage drop across the connection while ensuring a low current to avoid heating of solder balls by Joule effect. Figure 5 shows an example of the voltage drop at the moment of failure in the assembly.

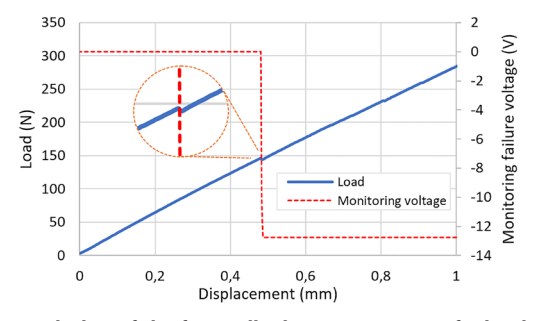


Figure 5: Evolution of the force-displacement curve of a loaded assembly (blue curve) and of the voltage drop (red curve) at the time of a connection failure

Test Procedure and Matrix

The equipment used is an electromechanical tensile test machine, Instron type 5500R. It is equipped with a 5 kN load cell and a flexural setup. For 4-point bending tests, the loading punch has been adapted. The test is displacement-controlled with a rate of 2 mm/min representative of the ramp-rates undergone by PCBAs during

handling. This rate was proposed based on the return on experience from operators working on the installation of thermal gap pads. Due to the low stiffness of the specimen compared to that of the test device, the displacement is done by the machine sensor.

Isothermal tests are carried out with the same apparatus, equipped with an Instron thermal chamber. This allows the temperature to be regulated at 125°C (electric heating), as well as at -55°C (nitrogen cooling). The temperature in the test area is regulated at +/-2°C. Once the temperature has been reached, a 10-minutes dwell time is observed to ensure good thermal homogeneity of the specimen.

The test matrix consists of 6 sets of tests, each with 20 (configurations 1 and 2) or 10 samples (Table 1). The basic configuration is 3-point bending with the SAC305 solder material, except for configuration 2 (SnPb36Ag2 material) and configuration 5 (4-point bending). Configuration 6 corresponds to tests after ageing at 125°C. The studies on the ageing of SAC305 solder alloy have shown that most of the effects on the mechanical behavior of the solder material are obtained during the first 200 hours of testing [7]. For this reason, the selected ageing time is 8 days (192 h).).

Table 1: Test matrix

| Config. # | Config. 1 | Config. 2 | Config. 3 | Config. 4 | Config. 5 | Config. 6 |
|--------------------------|-------------|-----------|-------------|-------------|-------------|------------------|
| Number of samples | 20 | 20 | 10 | 10 | 10 | 10 |
| Solder alloy | SAC305 | SnPb36Ag2 | SAC305 | SAC305 | SAC305 | SAC305 |
| Bending configuration | 3-points | 3-points | 3-points | 3-points | 4-points | 3-points |
| Displacement velocity | 2 mm/min | 2 mm/min | 2 mm/min | 2 mm/min | 2 mm/min | 2 mm/min |
| Temperature | 20°C | 20°C | -55°C | 125°C | 20°C | 20°C |
| Isothermal aging | No | No | No | No | No | 192h at 125°C |

FINITE ELEMENT ANALYSIS

The FEM analysis is performed using ANSYS Workbench 2020 R2 software. Considering the symmetries of the problem, 1/4th of the test vehicle is modeled to reduce computing time. A global-local approach using sub-modeling technique is used to assess the local PCB strain near the critical solder ball. The width of the local model is equal to half of the solder ball pitch. Figure 6 shows the coarse mesh of the global model and the fine mesh applied for the local model.

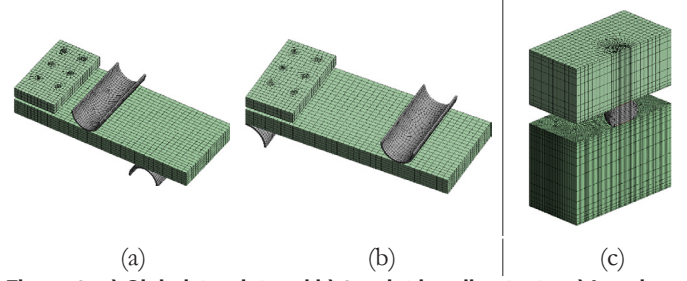


Figure 6: a) Global 4-point and b) 3-point bending tests. c) Local model depicting the critical solder ball

Temperature-dependent elastic properties are considered for the materials of the PCB and custom-made BGA. Young modulus is calculated considering the resin material as well as the fiberglass cloth thanks to an in-house numerical tool (AnCEA) allowing to calculate physical properties of any type of PCB stack-up. Since an aged configuration is tested (Table 1), it is important to consider

the aging-induced microstructural evolutions of SAC305 solder joints. Motalab studied the mechanical properties of aged SAC305 reflowed samples and derived the corresponding Young modulus using tensile tests data [7]. The Young moduli corresponding to the un-aged and 20 day-aged samples at 100°C are therefore considered in this study. The elastic modulus of SnPb36Ag2 solder alloy is obtained from the literature [8]. The punches are modeled as steel parts and the pads with copper using default material properties given in Ansys. Table 2 sums up the elastic properties considered for the FEM analysis.

Table 2: Elastic material properties used for the FEM analysis (*default value)

| Material | E (GPa) | v | Reference | |
|---|---|-------|-------------------|--|
| Panasonic 1755V + 7628 fiberglass cloth (PCB and custom-made BGA) | E(T) = -0.013 T($^{\circ}$ C) + 13.95 (-55 $^{\circ}$ C \le T \le 125 $^{\circ}$ C) | 0.16 | In-house software | |
| SAC305 | $E(T) = -0.27 T(^{\circ}C) + 53$ $(25^{\circ}C \le T \le 125^{\circ}C)$ | 0.33* | [7] | |
| SnPb36Ag2 | 31.4 | 0.33* | [8] | |
| Copper | 125 | 0.33 | Ansys | |
| Steel | 200 | 0.3 | Ansys | |

SAC305 solder alloy is also described as a viscoplastic material using Anand constitutive model. Motalab derived the Anand parameters corresponding to un-aged and 20 day-aged samples at 100°C using creep tests data [7]. The viscoplastic properties of SnPb36Ag2 solder alloy are given in [8]. Table 3 sums up the Anand parameters considered for the FEM analysis according to the solder material and the aging condition.

Table 3: Anand viscoplastic models used for FEM analysis

| Anand parameters | SAC305 unaged [7] | SAC305 aged 20 days at 100°C [7] | SnPb36Ag2 unaged [8] |
|----------------------|-------------------|----------------------------------|------------------------|
| s ₀ (MPa) | 16.33 | 6.37 | 56.33 |
| Q/R (K) | 9096 | 9096 | 10830 |
| A (s-1) | 3518 | 4145 | 1.49 x 10 ⁷ |
| ξ | 4 | 4 | 11 |
| m | 0.188 | 0.136 | 0.303 |
| h_0 (MPa) | 160000 | 122170 | 2640.75 |
| ŝ (MPa) | 24.64 | 22.41 | 80.42 |
| n | 0.015 | 0.0028 | 0.0231 |
| а | 1.79 | 2.25 | 1.34 |

The simulations on the global model are conducted to determine the overall behavior of the test vehicles under the different static bending conditions and identify the critical solder joint. The simulation considering the local model is then performed in order to calculate the local PCB strain ($\Delta ePCB$) near the identified critical solder joint for each imposed Z-displacement (Figure 7).

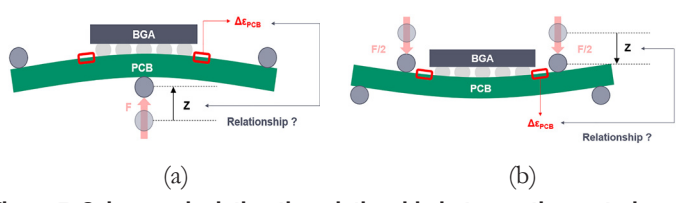


Figure 7: Schemes depicting the relationship between the central displacement and the local PCB strain for the a) 3-point bending and b) 4-point bending tests

RESULTS AND DISCUSSION

Static Tests

The mechanical behavior of the assemblies was evaluated using static bending tests during which we recorded the evolution of the applied load as a function of displacement and the electrical continuity of the circuit as a function of displacement. Figure 5 shows an example of these evolutions for a SAC305 assembly loaded at room temperature. We observe that the mechanical behavior of the system is roughly linear and that the stiffness variation at the moment of failure of a connection is very small. This observation is correlated to the numerical simulations. The average stiffness of 294.2 ±4.9 N.mm-1 also correlates with the numerical simulation results.

The Weibull distribution is one of the most widely used lifetime distributions in reliability engineering. It is a versatile distribution that can take on the characteristics of other types of distributions, based on the value of two parameters η and β . The scale parameter η , corresponds in our case to the displacement at which 63.2% of the assemblies will have failed and the shape parameter β represents the dispersion of the results (slope of the Weibull plot). Weibull curves shown in Figure 8 allow the comparison of the different test configurations.

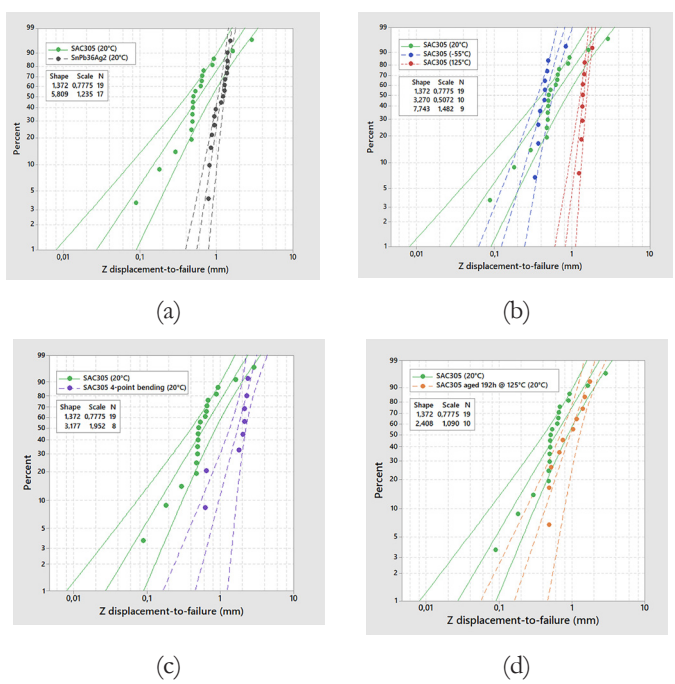


Figure 8: Weibull plots comparison of displacement-to-failure, a) SAC305 versus SnPb36Ag2, b) three tests temperatures for SAC305 configurations, c) 3-point versus 4-point bending test, d) after aging

We can observe that the displacement-to-failure is lower for the SAC305 alloy than for SnPb36Ag2, configurations 1 and 2 respectively. For the SAC305 alloy, the displacement at failure increases with temperature (config.1, 3, 4). It is also higher for the aged alloy case (config. 6) and for the 4-point bending configuration (config. 5) compared to the reference configuration

(config. 1). Figure 8.a compares assemblies made of SAC305 and SnPb36Ag2. The SAC305 configuration has a shape factor about 4 times lower than that of the lead alloy. This larger dispersion is often observed in mechanical fatigue under vibration or shock for electronic assemblies. This behavior can be explained by the microstructure of the alloys which is quite heterogeneous in the case of SAC305 and more homogeneous (on a mesoscopic scale) in the case of SnPb36Ag2 [9]. If we focus on the temperature (Figure 8.b), we can see that the test at 20°C shows a singular behavior, probably due to some experimental uncertainties (values of shape parameters increasing with temperature). For the 4-point bending tests (Figure 8.c), it is consistent to measure larger displacements at failure, particularly because this test is less severe than the reference configuration. However, it would appear that there are "outliers". These points appear to be abnormally low/high or outside the 95% confidence intervals. As failure analysis on the points that appear to be outliers could not be done, we did not discard them. For the ageing study, the results are consistent (Figure 8.d). Aging for 192 h at 125°C modifies the microstructure of the SAC305 solder balls. This results in the coalescence of the internal Ag3Sn IMCs leading to an easier movement of the dislocations which are no longer blocked by these IMCs whose diameter is larger [10].

Failure Analysis

The failure analysis was based on micrographic cross-sections and observations using optical microscopy and scanning electron microscopy (SEM). Energy Dispersive Spectroscopy (EDS) is also used to analyze the chemical elements in the assembly. The samples are first encapsulated in a resin material and then polished according to an appropriate process. In the figures 9, 10 and 11, the PCB is located at the bottom of the solder ball, while the component is at the top. We observe failures on the PCB side or on the component side according to the loading conditions. Most of the failures are located on the PCB side for the SAC305 and SnPb36Ag2 specimens in 3-point bending configuration at 20°C (config. 1 and 2) (Figure 9), but also for the aged SAC305 (config. 6).

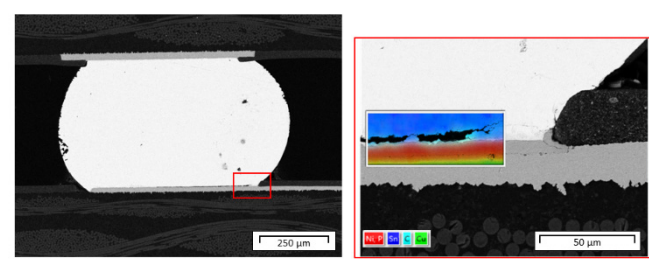


Figure 9: Fracture on the PCB side located at the IMC/ENIG surface finish for SAC305 alloy at 20°C (config 1.)

For the other configurations (number 3, 4 and 5), the failures are preferentially located on the component side, although there are exceptions, for example in the case of the aged SAC305 in figure 10. Nevertheless, in all cases, the fracture is initiated at the interface between the (Cu,Ni)6Sn5 intermetallic layer and the ENIG surface finish. This description can be seen for the 20°C tests on SAC305

(config.1, Figure 9) and for the 125°C test aged specimens (config. 4, Figure 10).

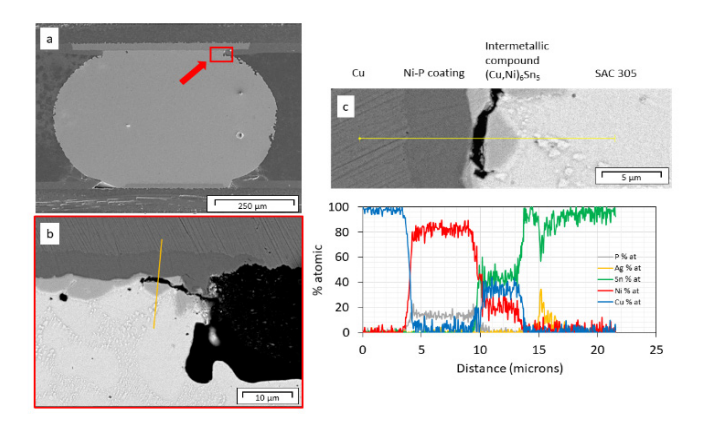


Figure 10: Fracture on the component side located at the IMC/ENIG surface finish for SAC305 alloy at 125°C (config 4.). The EDS analysis allow to distinguish the several chemical elements composing the solder joint interface

In some fewer cases, it is possible to see a fracture of the copper trace on the PCB side as shown in Figure 11.

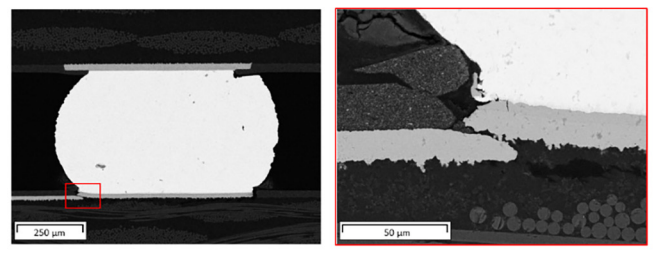


Figure 11: Fracture on the PCB side located at the cooper trace for SAC305 alloy at 20°C (config 1.)

Finite Element Analysis

In order to be able to assess the risk of solder ball failure under static bending for any type of PCBA, it is important to convert the measured central displacement-to-failure into a criterion which is not boundary conditions-dependent. As a result, it was decided to calculate the local PCB strain near the critical solder joints since it is a criterion that gives an indirect evaluation of solder joints damage. An equivalent PCB strain is calculated in Ansys considering the following equation:

$$\Delta \varepsilon_{PCB} = \sqrt{\Delta \varepsilon_x^2 + \Delta \varepsilon_y^2 + \Delta \varepsilon_z^2}$$

Each tested configuration was modeled and several simulations were performed in order to obtain the relationships between the imposed central displacement and the local PCB strain near the critical solder joints. Figure 12 shows the test vehicle deflections calculated with the global 3-point and 4-point bending models.

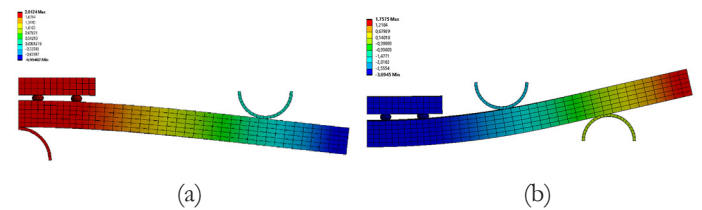


Figure 12: Calculated Z-displacement corresponding to a) the 3-point and b) 4-point bending tests

The global model allows to determine the location of the critical solder joint of the test vehicle. The global model results show that the critical solder ball is located at the furthest distance from the neutral point. The local model focuses on this specific solder ball and by importing the boundary conditions from the global model when the maximum deflection is reached, it is possible to calculate the maximum local PCB strain (Figure 13).

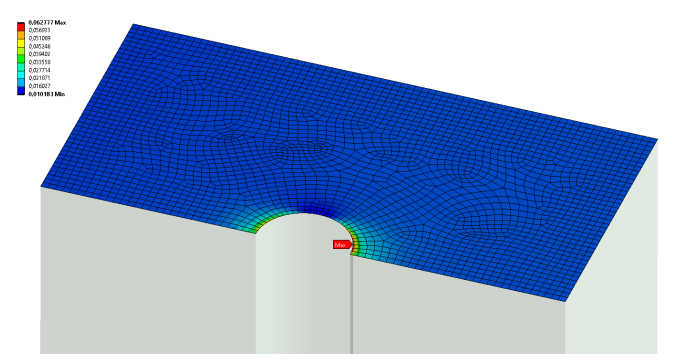


Figure 13: Calculated local PCB strain near the critical solder joints after PCBA bending

In order to take into account potential model singularities (geometry and change in material properties) and to get results independent of the mesh, an averaged PCB strain in the most deformed area was calculated according to the following equation:

$$\Delta \varepsilon_{PCB_ave} = \frac{\sum_{i} \Delta \varepsilon_{PCB_i} \times V_{i}}{\sum_{i} V_{i}}$$

with $\Delta \epsilon_{PCB_{\underline{i}}}$ and V_i , the PCB strain and the volume of the i^{th} element respectively.

As the PCB behaves elastically, there is a linear relationship between the applied central deflection and the calculated PCB strain (Figure 14). The slope corresponding to the 4-point bending test is obviously quite different from those corresponding to the 3-point bending tests. The graph shows that there is a negligible influence of the PCB material properties on the local PCB strain. Regardless of the temperature, the relationships between the central displacement and the local PCB strain are virtually identical.

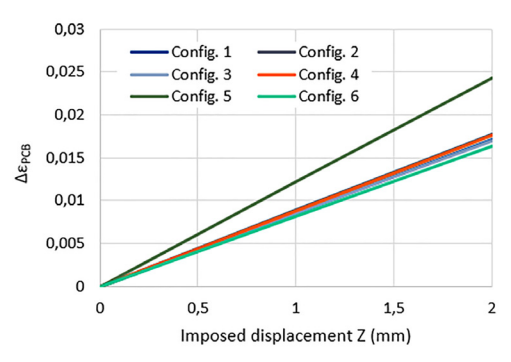


Figure 14: Relationship between the imposed displacement and the local PCB strain determined after FEM analysis

However, with the constitutive viscoplastic model considered for the aged SAC305 solder balls, the curveplotted shows a slightly smaller slope, which means that for the same imposed central displacement, the local PCB strain near the critical solder ball is less important when the test samples are aged at 125°C during 192 hours. During aging, Ag₃Sn intermetallic compounds coalesce so that dislocations can move more easily [10]. Since solder joints become less resistant to deformation, one can assume that the local stiffness at the location of the BGA decreases and therefore the PCB curvature near the critical solder ball would be smaller than with the unaged SAC305 properties: $\kappa_{\text{without aging}} > \kappa_{\text{with aging}}$ (Figure 15). As the PCB strain can directly be approximated from its thickness (t) and the curvature (κ) with the equation

$$\Delta \varepsilon_{PCB} = \kappa.t/2,$$

it would be consistent to calculate smaller local PCB strain with the FEM analysis representative of the aged test samples.

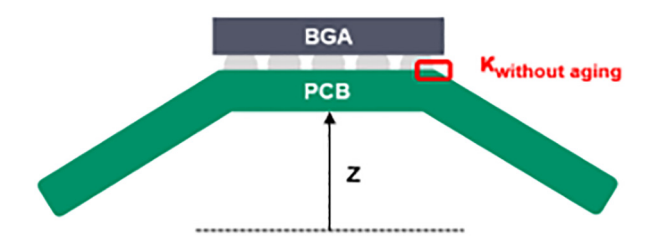


Figure 15: Schematic views of the BGA assemblies a) without aging and b) after aging

Thanks to the obtained relationships, it is possible to correlate the central displacement-to-failure with its corresponding PCB strain. The calculated PCB strain data could therefore be a help for designers who want to assess the criticality of a design when static PCBA bending can occur. Table 4 sums up the Weibull parameters corresponding to the local PCB strain-to-failure distribution.

Table 4: Weibull parameters corresponding to the PCB strain-tofailure distribution for each tested configuration

| Config. # | 1 | 2 | 3 | 4 | 5 | 6 |
|---------------------------|--------|--------|--------|--------|--------|--------|
| Scale: η (Δερcb_63.2%) | 0.0065 | 0.0112 | 0.0043 | 0.0131 | 0.0237 | 0.0089 |
| Shape: β | 1.3 | 6.3 | 3.3 | 7.7 | 3.1 | 2.4 |

It is also interesting to note that the obtained solder ball equivalent total strain contours are correlated with optical microscopy observations made on cracked BGA assemblies (Figure 16). For the 3-point bending test, the crack is located on the PCB side at the interface between the intermetallic layer and the ENIG surface finish.

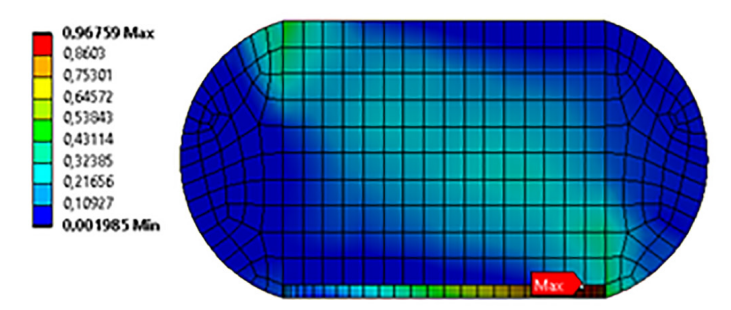


Figure 16: Total equivalent strain contours in the critical solder ball (3-point bending test)

CONCLUSION

A specific test vehicle has been developed to assess the mechanical durability of SAC305 and SnPb36Ag2 BGA assemblies under flexural loading. In order to take into account the position of the components on the PCB, i.e. whether they are on the convex or concave side of the PCB, 3-point bending tests have been conducted at -55°C, 20°C and 125°C and 4-point bending tests at 20°C. A set of SAC305 test samples has also been aged at 125°C during 192 hours to assess the influence of solder joints microstructural evolution on the propensity of interconnects to crack during bending. Bending tests are performed at a ramp-rate of 2 mm/min until the daisy-chained BGA assemblies fail. Weibull plots depicting the distribution of the central displacement-to-failure show that:

- As temperature increases, the durability of SAC305 solder joints increases,
- The durability of aged SAC305 solder interconnects is slightly better than the durability of unaged SAC305 solder joints,
- SnPb26Ag2 outperforms SAC305,
- The durability of SAC305 BGAs on the concave side of the PCB (surface in compression) is higher than the durability of SAC305 BGAs on the convex side of the PCB (surface in tension).

These results were post-treated in order to be able to consider a criterion which is not boundary conditions-dependent. As a result, FEM analysis was conducted and the test vehicle was modeled using a global-local approach. Solder ball strain contours were calculated and correlated with the observations made during failure analysis. The local PCB strain near the critical solder joint was calculated for each test configurations in order to establish the relationship between the central displacement and the local PCB strain. It was then possible to determine the Weibull parameters of the PCB strain-to-failure distribution. This study provides the necessary data

to help designers who have to ensure that their PCBA designs are not at risk when subjected to static bending.

Future Work

Static bending of PCBAs can occur and remain throughout the electronic equipment life cycle. While the static load remains, the PCBAs embedded in the equipment can also be subjected to harsh environments such as large temperature variations as well as vibrations and shocks. It is therefore important to assess the influence of PCBA static flexural loading on SAC305 solder joints fatigue under thermal cycling and cyclic mechanical loading.

Future work will therefore consist in conducting thermal cycling tests on "flat" and bent BGA assemblies (convex and concave side). New test vehicles will be designed since the current custommade BGAs have the same material as the PCB substrate. There is therefore no Coefficient of Thermal Expansion (CTE) mismatch between the component and the PCB and solder joints will not fail.

REFERENCES

- L.B. Tan, S.K.W. Seah, E.H. Wong, Xiaowu Zhang, V.B.C. Tan, C.T. Lim, "Board level solder joint failures by static and dynamic loads", Proceedings of the 5th Electronics Packaging Technology Conference, pp. 244-251, 2003.
- A. Bansal, S. Yoon, V. Mahadev, "Flexural strength of BGA solder joints with ENIG substrate finish using 4-point bend test", SMTA Pan Pacific Microelectronics Symposium, 2005.
- 3. F. Song, K. Newman, C. Yang, S.W. Ricky Lee, "Investigation of lead-free BGA solder joint reliability under 4-point bending using PWB strain-rate analysis", 11th Electronics Packaging Technology Conference, pp. 863-868, 2009.
- 4. L. Long, G. Li, X. Liao, B. Xie, X. Shi, "Dynamic bending test and simulation of PBGA packages", International Conference on Electronic Packaging Technology & High Density Packaging, pp. 859-863, 2011.
- 5. S. McCann, T. Lee, S. Ramalingam, "Finite Element Modeling methodology for monotonic bend test of flip-chip BGA package", 70th Electronic Components and Technology Conference, pp. 2086-2091, 2020.
- 6. R.J. Roark, "Formulas for stress and strain", New York: McGraw-Hill, 1975.
- 7. M. Motalab, "A constitutive model for lead free solder including aging effects and its application to microelectronic packaging", PhD Dissertation, Auburn University, 2013.
- G. Wang, Z. Cheng, K. Becker, J. Wilde, "Applying Anand model to represent the viscoplastic deformation behavior of solder alloys", Journal of Electronic Packaging, Vol. 123, No. 3, pp. 247-253, 2001.
- J-B. Libot, "Méthodologie d'évaluation de la durée de vie des assemblages électroniques sans plomb en environnements thermique et vibratoire". PhD thesis, Univ. Toulouse, INPT, 2017.
- J-B. Libot, J. Alexis, O. Dalverny, L. Arnaud, P. Milesi, F. Dulondel, "Microstructural evolutions of Sn-3.0Ag-0.5Cu solder joints during thermal cycling", Microelectronics Reliability, Vol. 83, Issue 2, pp. 64-76, 2018.

BIOGRAPHIES



O. Dalverny received the M.Eng. degree from the National Engineering school of Tarbes, France, the M.S. degree from the University of Bordeaux, France, in 1993. In 1998, he obtained a Ph.D. in Mechanics from the University of Bordeaux, France. His thesis work focused on the study of high temperature sliding behaviour of a ceramic material. He is currently a Professor at National Engineering school of

Tarbes, where he has been working in the Metallurgy, Mechanics, Structures, and Damage research group of the Mechanics, Materials and Processes department. His current research focuses on the non-linear behaviour of materials and structures, including multimaterial assemblies and packaging applications.



J. Alexis received the M.Eng. degree from the National Engineering school of Tarbes, France, the M.S. degree from the National Polytechnic Institute of Toulouse, France, in 1996. In 2000, he obtained a Ph.D. in material science from the National Polytechnic Institute of Toulouse, France. His thesis work focused on the mechanical behaviour of new surface treatments. He is currently a Professor at National Engineering school of Tarbes, where

he has been working in the Metallurgy, Mechanics, Structures, and Damage research group of the Mechanics, Materials and Processes department. His current research focuses on the study of gradient materials (coatings, brazing, welding, and additive manufacturing).



Jean-Baptiste Libot obtained his Master's degree in Material Engineering from the National Polytechnic Institute of Toulouse in 2011. The same year, he also obtained a Research Master diploma in Materials, Nanomaterials and Multi-Materials science. Then he joined Airbus Group and work for two years at the Center for Advanced Life Cycle Engineering (CALCE) in the field of Electronic Reliability.

He obtained his PhD from the National Polytechnic Institute of Toulouse in Mechanical and Material Science in 2017. He now works as an Electronic Materials & Processes Engineer at Safran Electronics & Defense.